Dynamic Voltage Restorer (DVR) System based on Two Port Hybrid High Gain Buck Boost Converter for Reducing Energy Consumption

D C Kumaresan[1*], Dr.P.Selvan[2]

[1]*Research Scholar, Department of EEE, Karpagam University, Coimbatore-641021, Tamilnadu, India*
[2]*Professor and Head, Department of EEE, Erode Sengunthar Engineering College, Tamilnadu, India*

Abstract: *Energy consumption and utilities have increased in the last two decades due to diversified applications in the field of science and engineering. Thus, energy saving have become an active research. It has become an essential criterion to take out system faults to ensure the efficient functioning of the overall system. The power quality issues concerned with voltage sag and they frequently cause serious power interruptions, if suitable care will not be taken in time. This work presents a novel photovoltaic fed Dynamic Voltage Restorer (PV-DVR) model to alleviate deep voltage sags and outages on a low voltage residential distribution system. The application of low step up and high step up DC-DC converters used in the existing DVR system results in high conversion loss. Moreover, two control loops are required to control the two separate converters which results in higher control complexity. Thus, in this proposed work, two port hybrid high gain buck boost converter (TPHGC) is integrated in the existing PV-DVR system. Two converters used in the existing system are replaced with single battery charging bidirectional converter. Simulation results are presented to validate the advantage of the proposed system.*

Keywords: *DVR; Reactive Power; Compensation; Controller; Maximum Power Point Tracking (MPPT) algorithm*

1. Introduction

This Dynamic Voltage Restorer (DVR) is cost effective system model as it mitigates voltage swells, sags as well as outages by determining the correct voltage quality level needed by sensitive loads such as mobile phones, laptop, TV, etc [1,2]. For small industries, especially, domicile devices, DVR has become the most preferred and positive solution. Industries and residential areas face power problems and fluctuations in power supply primarily due to the voltage swells that are generally of a short duration, sags and other associated power breaks that are of a longer duration [3, 4, 5].

The concept illustrated in [6] is the application of DVR to address the issues of voltage sags and outage improvement in the absence of a PV system. Figure 1 shows a series injection transformer's architectural design and its rating [7]. There are several research works that have been conducted that focus on the design and control of DVR [8]. The on-line kind of DVR as discussed in [9] has been offered to compensate the system's voltage sag. In the electrical distribution system, the DVR which does not have a PV system, is additionally propped up by an energy storage tool which is the super capacitor and it aids in power quality enhancement as presented [10]. The PV operated DVR here plays the role of compensating the system's voltage sag as presented in [11]. In the above mentioned DVR models, there are no monetary customer benefits. So, this paper proposes a PV-DVR model which overcomes the limitations of the above mentioned models. PV-DVR work presented in [12] is the main motivation behind this research work. The main objective of this research work is to design a modified converter for the existing PV-DVR system [12].

The conventional PV-DVR block diagram [12, 13] is shown in figure 1. In this existing PV_DVR system, two types of converters namely low step up and high step up have been used [14,15]. To control the low step up DC–DC converter, the P&O MPPT algorithm is used [15, 16, 17]. Similarly, in order to control the high step up DC-DC converter, outer voltage control based closed loop system is used. These two conversions results in high conversion loss, as two converters are used in the existing system. The battery presented in this existing system charges through low step up converter where as the discharging operation takes place through high step up converter. Thus, two converters are used in this existing system. Moreover, a charging controller has also been used to define the state of charge (SOC) of the battery as shown in Fig 1.

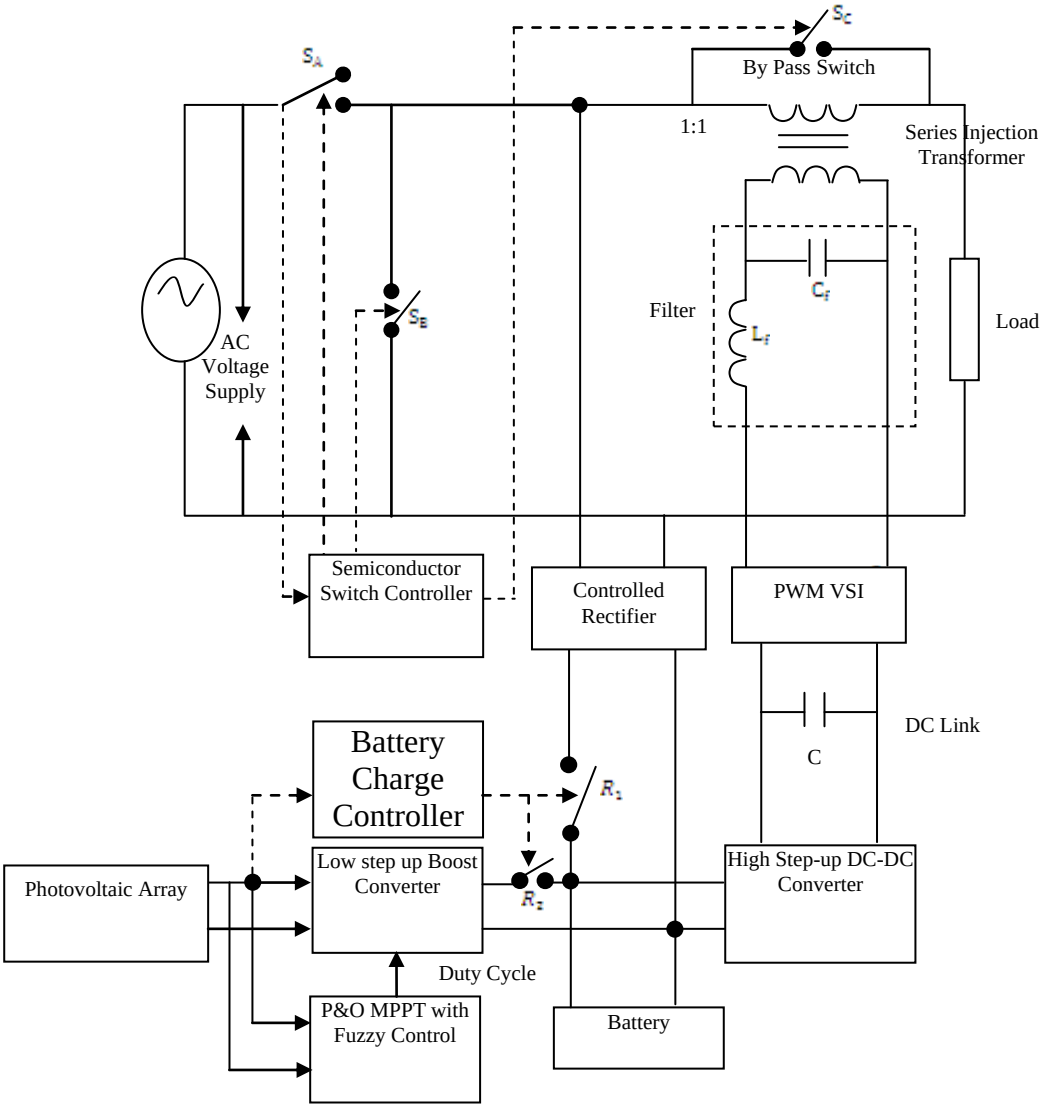

Fig.1. Block diagram of conventional PV-DVR

Thus, three controlling techniques have been used here. The battery charger controller with two bypasses switches and has been used in the existing system. Considering a scenario, wherein the battery gets fully charged, the excess voltage from the PV array may not be utilized by the battery which results in wastage of power. Thus, in the existing system, the efficiency gets reduced with increased control complexity. On the other hand, the cost and system size also gets increased.

In this research work, in order to overcome the drawbacks of the existing system, a two port hybrid high gain buck boost converter (TPHGC) has been integrated in the existing PV-DVR system. In this proposed PV-DVR system, PV array and battery represent the two port section. Two converters used in the existing system are replaced with single battery charging bidirectional converter as shown in Fig 2.

The proposed PV-DVR system operates in three modes of operations as described below.

- PV Power = Output Power (Ideal)
- PV Power > Output Power (Battery Charging)
- PV Power < Output Power (Battery Discharging

The battery charge control logic is shown in Table 1 below.

Table 1: Battery Charge Control

PV voltage in volts	Control Signal		Battery charging unit
	R_1	R_2	
>6	0	1	PV array
<6	1	1	Rectifier and PV array

2. System Description

The Fig. 2 shows the proposed PV-DVR architectural design with the novel TPHGC. The proposed system comprises of the battery, a PV array, PWM inverter, and series injection transformer, TPHGC and semiconductor switches marked as, & .

Normally and are closed and open when grid voltage is in a state of normal. On the other hand, when and are open and is closed, the system acts in UPS mode. Similarly, sag compensation mode occurs when is closed, & are open.

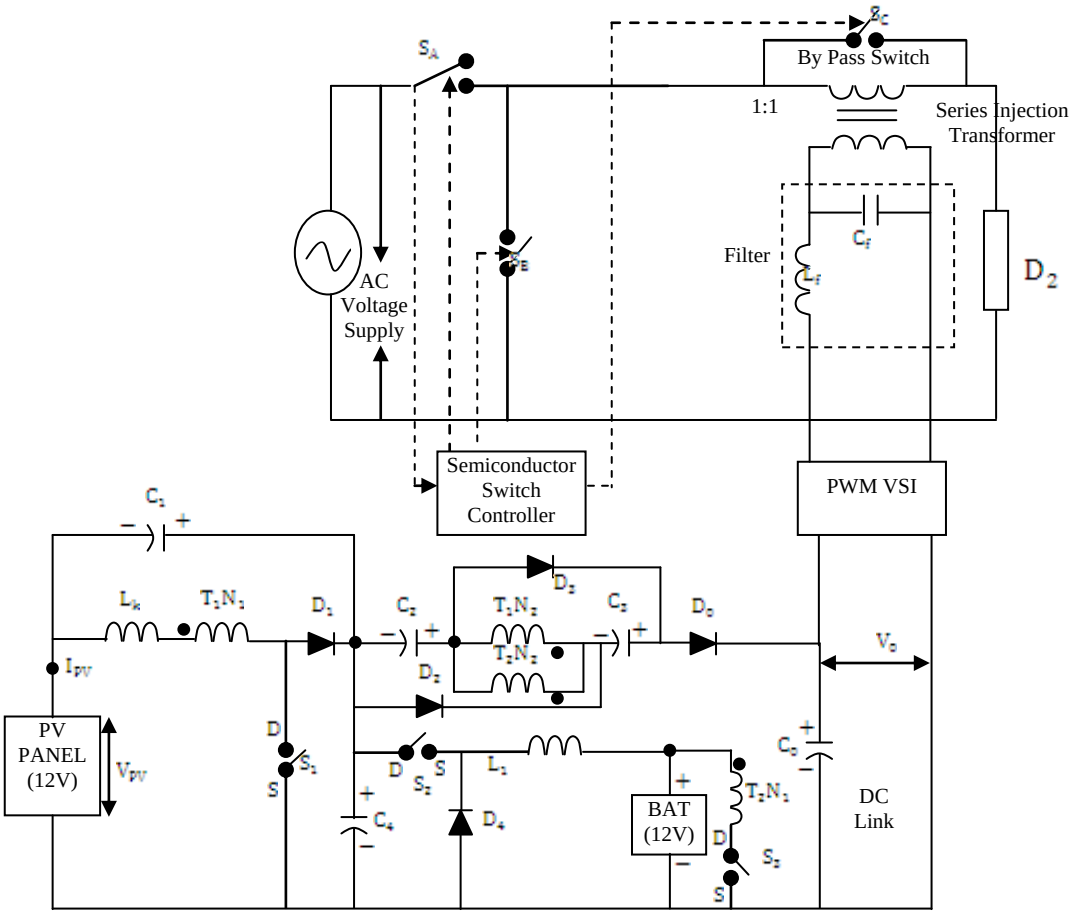

Fig.2. Proposed Two Port Hybrid High Gain Buck Boost Converter based PV-DVR system

Table 2: Control Signal for S_A, S_B and S_C

Supply Voltage in %	Control Signal			Mode of Operation
	S_A	S_B	S_C	
100	1	0	1	idle
<100	1	0	0	DVR
0	0	1	0	UPS

Table 2 shows the semiconductor's control signals as switches , & . The functioning of the proposed PV-DVR in three modes is discussed in detail:

The idle or maintenance mode: The PV-DVR during this mode is completely disconnected in the semiconductor switch course. This is done in the secondary phase by passing the injecting transformer wherein maintenance is required by the DVR.

The compensation mode also known as DVR mode: Proposed PV-DVR in the compensation mode is used to bring in a state of voltage regulation in the load side. In this process the load basically compensates voltage sags which are configured sequentially in the series injection transformer.

Uninterruptible Power Supply (UPS) mode: During the UPS mode, PV-DVR series injection transformer is basically configured again as parallel, so that it supplies the load with an uninterruptible power supply both during the day as well at night.

2.1. Mode of operation

i.PV power=Load power

Five Modes of operation has been presented for the scenario PV power = Load Power as shown in Fig 3. This mode of operation clearly describes the condition when the load power is met (satisfied) by the PV power.

In this mode (S_1), initially the current from PV flows through the transformer and the switch so that it neutralizes. Thus, the current flow through the transformer , creates a flux which in turn generates the current flow in the secondary winding of the transformer . At this point of time, two circulating paths are created which charges capacitor and .

The current flowing path for charging the capacitor is initiated from the secondary winding of the transformer and charges the capacitor then flows through the diode which completes the circulating path. Similarly, the current flowing path for charging the capacitor is initiated from the secondary winding of the transformer and flows through the diode and then charges the capacitor which completes the circulating path.

Mode 1

The initial current flowing path of Mode 1 is same as discussed in Mode 0. At this time, extra current in the inductance flows through the capacitors and and energizes the secondary winding of the transformer . Then the current flows through capacitor . Thus, the capacitor , and are in series and the voltage is stored in capacitor which culminates in a high gain mode operation.

At this point, a circulating path is created which charges the capacitor through the capacitor and gets neutralized at PV.

Mode 2

In this mode is in OFF condition. This mode is almost similar to the mode 1, which is based on the linear discharge of as shown in Fig 3(c).

Mode 3

This mode is also called as leakage inductor discharge mode. This is same as the mode 2 but leakage inductance of the transformer gets discharged through diode and stores the voltage across the capacitor and gets neutralized at PV as shown in Fig 3(d).

Mode 4

In this mode, capacitor is in a fully discharged condition. Now, the voltage stored in the capacitor gets discharged and energizes the transformer and flows through the diode and gets neutralized. At this point, current through the transformer creates a flux which in turn generates the current flow in the secondary winding of the transformer which further produces two circulating paths ((capacitor charging) as mentioned in mode 0 as shown in Fig. 3(e).

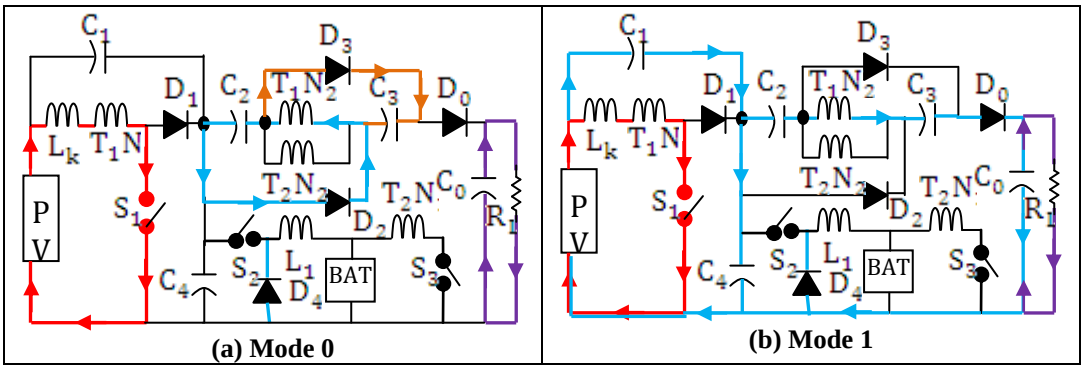

(a) Mode 0 **(b) Mode 1**

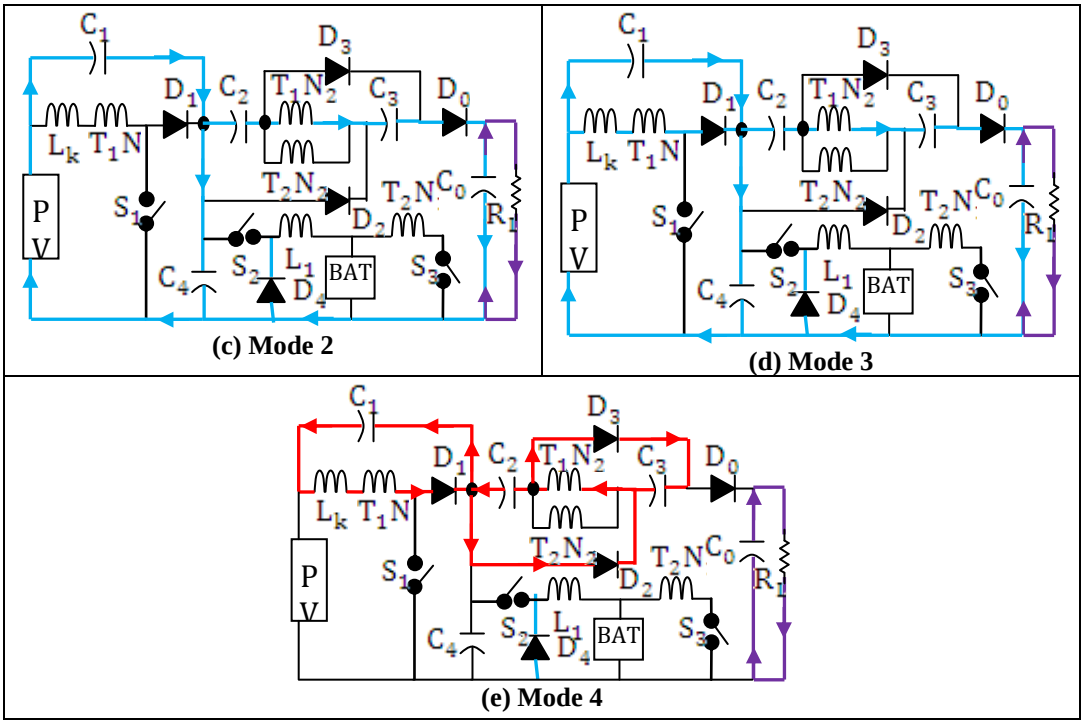

Fig.3. PV power=Load power

ii.PV power>O/P power

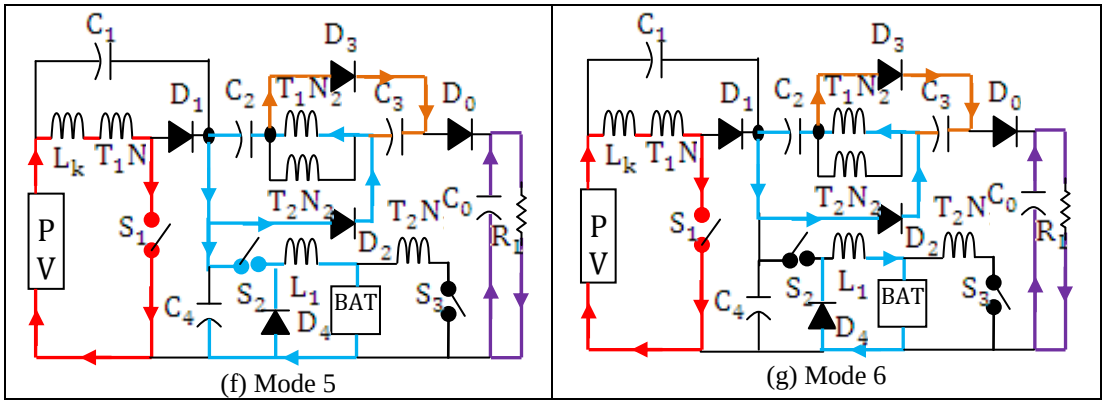

Fig.4. Mode of operation PV power>Load power

iii.PV power<O/P power

In this 'PV power<O/P power' condition, the generated PV power is lesser than the load power and now, in order to meet the load demand, the stored power from the battery is discharged to meet the required load demand based on the controlling technique as shown in Fig 5. At this discharging condition, boost operation is carried out to meet the load demand.

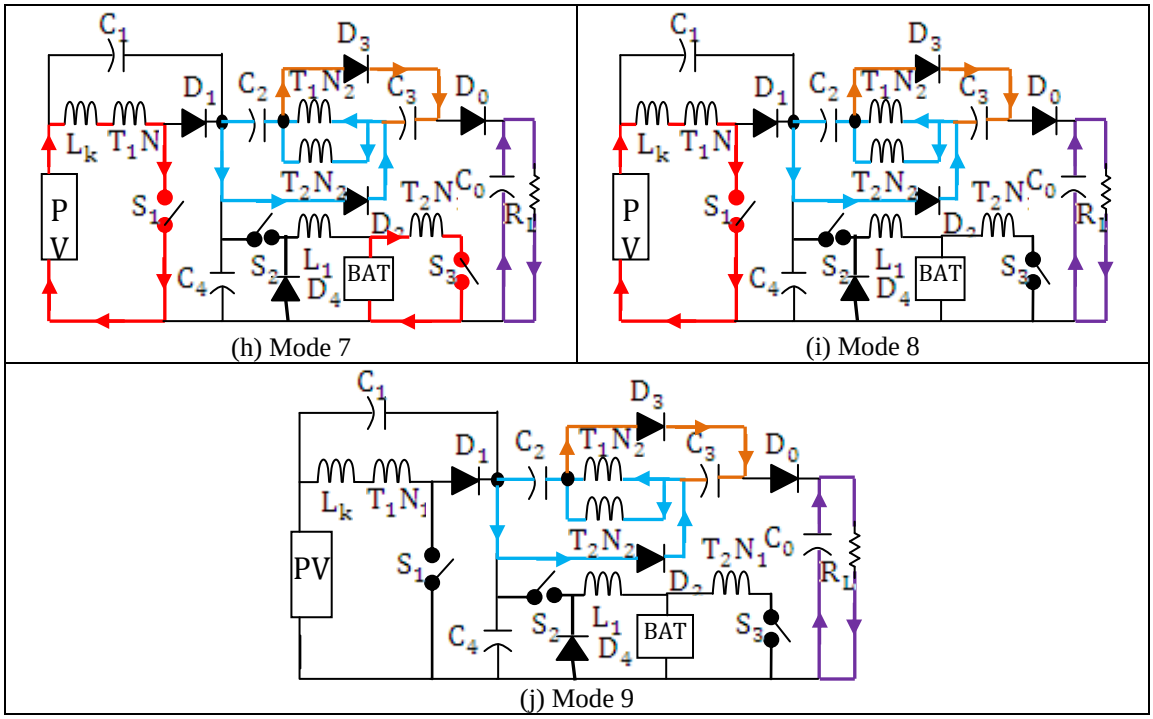

Fig.5. Mode of operation PV power<Load power

All modes of operations (Mode 0 to Mode 4), occurred in PV power=load power condition, is same for this operation. This mode of operation initiates with switch in ON condition. Thus, the current from the battery flows the primary winding of the transformer and then flows through the drain source of switch and gets neutralized.

Due to the current flow in the primary winding of the transformer , flux is created at the secondary winding of the transformer . Based on the previous modes, when the switch is in ON condition, the flux is generated at the transformer. Now, the flux generated at and , simultaneously charges the capacitors and respectively which acts in series connection and support the load demand as shown in Fig 5 (hmode 7).

In mode (8), switch is in OFF condition, remaining flux in transformer gets discharged and simultaneous, switch becomes OFF state which in turn makes the remaining flux in transformer to get discharged fully to support the load demand. The end of this cycle leads to the beginning of the next cycle (PV power = Load power).

2.2. Two Port Hybrid High Gain buck boost converter (TPHGC) control

In this MPPT conversion, P&O algorithm has been used for attaining the maximum power from the PV panel. The working of this P&O algorithm is mainly based on voltage and power. P&O algorithm works on the principle that, if there is increase in power, then the perturbation is maintained in the same direction and on the other hand, if there is decrease in the power, then the perturbation should be maintained in the opposite direction. This process is iterated until the maximum power point is reached.

A triangular carrier signal is generated with a switching frequency of 10 KHz as depicted in figure 6 (a). Duty cycle from the P&O algorithm and the carrier signal is compared to generate the PWM pulse. Based on this control operation, the PV voltage is boosted up through the MPPT to meet up the load voltage demand.

Figure 6(b) shows the outer voltage control with battery charging and discharging control loop. The battery charging and discharging is based on the load voltage. Thus, when the load voltage is high, the battery discharging operation is carried out by controlling the switch . On the other hand, when the load voltage is lower, the battery charging operation is carried out by controlling the switch which is clearly depicted in figure 6(b).

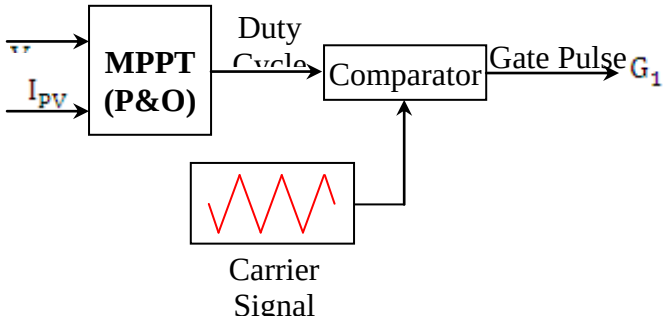

(a) Maximum power point tracking (MPPT) Control

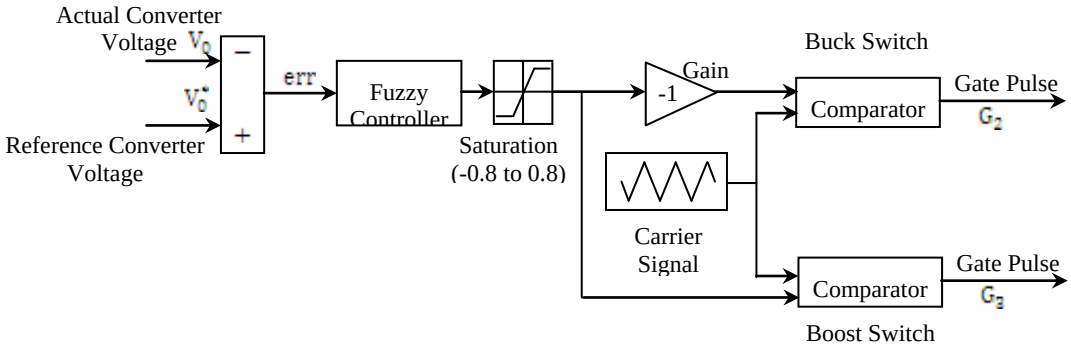

(b) Outer voltage Control Loop
Fig.6. Closed Loop Control of TPHGC

In this work, the actual and reference TPHGC voltage is compared and the output error is given to the Fuzzy controller for controlling operation. The voltage error from the proposed converter is taken as feedback to control the dc link voltage of the inverter. Thus, with this closed loop control system, the input voltage of inverter in the DVR is maintained constant.

FLC has two inputs which are: error and the change in error, and one output feeding to the pulse width modulation to control the DC-to-DC converter. The two FLC input variables error E and change of error CE at sampled times k defined by:

$$\text{Error}(k) = \frac{P(k)}{V(k)} \qquad (1)$$

Where P(k) is the instant power of the photovoltaic generator. The input error (k) shows the load operation point at the instant k which is located on the left or on the right of the maximum power point on the PV characteristic, while the input CE (k) expresses the moving direction of this point. The fuzzy inference is carried out by using Mamdani method, FLC for the Maximum power point tracker. FLC contains three basic parts: Fuzzification, Base rule and Defuzzification.

The output error from the controller is limited through a saturation limit unit which is assigned between (-0.8 to +0.8). In this work, a positive carrier signal is generated with 0 to 1 amplitude. Now, when the error output is negative, then error is multiplied with the negative Gain factor. Now, the negative error and the negative gain are multiplied to generate a positive error and are compared with the positive carrier to generate a gate pulse which acts in buck switching (charging) mode.

On the other hand, when there is positive error from the controller, then error is compared with the positive carrier signal and there is no need to multiply the gain factor in that scenario. Now, the positive error is compared directly with the positive carrier to generate a gate pulse which acts in boost switching (discharging) mode. Thus it may be inferred that the gate pulses and are always in inverse active mode wherein when switch is ON, switch would be in OFF state and vice verse.F21

2.3. Photovoltaic array modelling

A system which comprises of solar cells that produce electricity through the process of conversion of sunlight forms a PV array or a photovoltaic array. Through the MPPT algorithm, new efficient solar cells have been developed which has led to the increase of the solar panel with an alternate renewable source of energy. The PV array along with the MPPT methodology through the low step up DC converter in the proposed DVR has become the DVR inverter's DC voltage source. This lies between DC link's battery bank and the PV.

Designing of the PV array is carried out by deploying the photovoltaic cells' basic equations along with solar irradiation level and this effects the change in temperature [18,19]. The PV cell's output voltage is basically one of the photo current's functionalities and which is primarily determined by the amount of load current which in turn depends on the level of solar radiation [20]. PV cell output voltage is calculated as per the following:

$$V_c = \frac{AkT_c}{e}\ln\left(\frac{I_{ph} + I_0 - I_c}{I_0}\right) - R_s I_c \quad (2)$$

$$V_{PV} = V_c \times N_s \quad (3)$$

$$I_c = \frac{I_{pv}}{N_p} \quad (4)$$

Here 'e' refers to the electron's charge $(1.602 \times 1$, denotes the output voltage of PV cell in volts, refers to the reverse saturation current of diode $(48.10 \times 10$ k is Boltzmann constant (1.38 J/0K), is the cell output current in A, is the number of series cell (9), is the cell internal resistance (0.2 A refers to the curve fitting factor (1.23), is the operating temperature of the reference cell (25 0C), is the output voltage of PV array, is the photo current in A (8.07 A), is the output current of the PV array and is the number of parallel cells (6).

2.4. DVR Fuzzy controller

The control scheme used to maintain a constant voltage magnitude at the load point, under system disturbance, is shown in Fig 7.

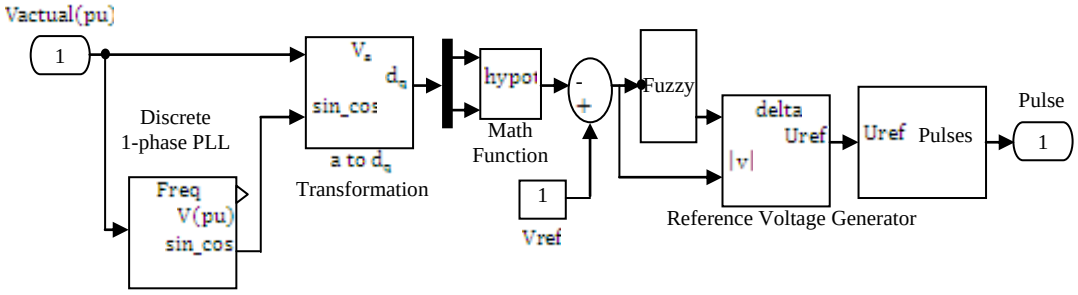

Fig.7.Control structure of DVR

Fig 8 shows the fuzzy logic controller. In the proposed controller, a discrete single phase PLL is used to track the phase angle of the source voltage to perform the parks transformation on the measured single phase voltage.

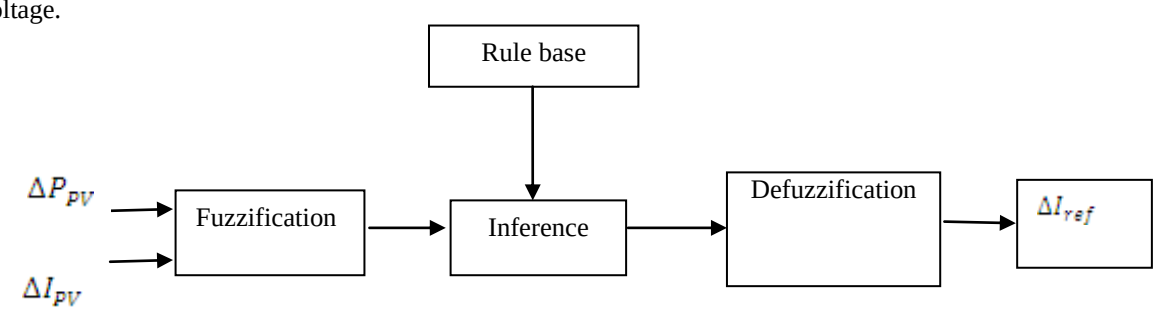

Fig.8. The Fuzzy Logic Controller

The measured p.u. value of supply voltage is converted into |Vs|, and the error is obtained from the difference of |Vs| and reference voltage ( ). The fuzzy controller designed by the processes of error and generates required angle d to drive the error to zero. The modulating angle d is applied to the reference voltage generator to generate the for the Sinusoidal Pulse Width Modulation (SPWM). The reference voltage calculation is obtained by the following equation

$$V_{ref} = |V| * \sin(\omega t + \delta) \quad (5)$$

The generated is utilized to produce switching pulses for VSI. The basic idea of SPWM is to compare a sinusoidal control signal ( ) of normal frequency 50 Hz with a triangular carrier waveform ( ) with 20 kHz signal to produce the PWM pulses. When the control signal is greater than the carrier signal, the switches are turned on, and their

counter switches are turned off. The output voltage of the inverter mitigates the voltage sag, swell and outage.

MPPT using Fuzzy Logic Control gains few advantages of better performance, robust and easy design. Besides, this technique does not need the knowledge of the exact model of system. The main parts of FLC, fuzzification, rule-base, inference and defuzzification, are shown in Fig. 8. In the proposed system, the input variables of the FLC are the change in PV array power (ΔPpv) and the change in PV current (ΔIpv), whereas the output of FLC is the magnitude of the change of boost converter current reference (ΔIref). The current reference is the command for controlling the current drawn from the PV. The equations for and are given as follows:

$$P_{pv}^{k} = V_{pv}^{k} \cdot I_{pv}^{k} \quad (6)$$

$$\Delta P_{pv}^{k} = P_{pv}^{k} - P_{pv}^{k-1} \quad (7)$$

$$\Delta I_{pv}^{k} = I_{pv}^{k} - I_{pv}^{k-1} \quad (8)$$

In the proposed design, the universe of discourse for the first input variable (ΔPpv) is assigned in terms of several linguistic variables by using seven fuzzy subsets, which are denoted by NB (negative big), NM (negative medium), NS (negative small), Z (zero), PS (positive small), PM (positive medium) and PB (positive big). The membership functions for the variable are shown in Fig.9. Fig. 10 and 11 shows the universe of discourse for the second input variable (ΔIpv), which is classified into 3 fuzzy sets, namely, Negative (N), Zero (Z) and Positive (P)

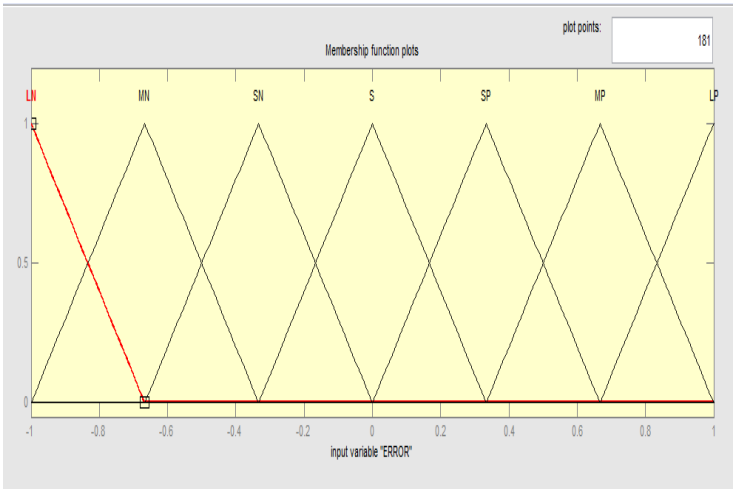

Fig. 9. Membership function used for input variable “error”

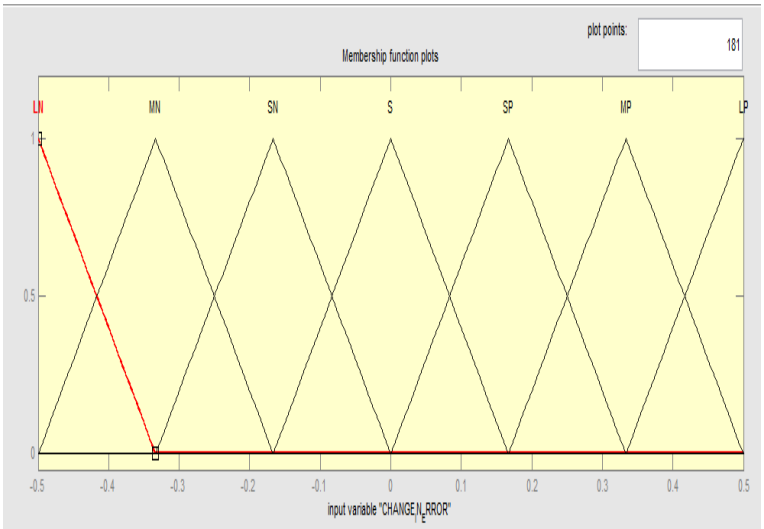

Fig. 10. Membership function used for input variable “Change in Error”

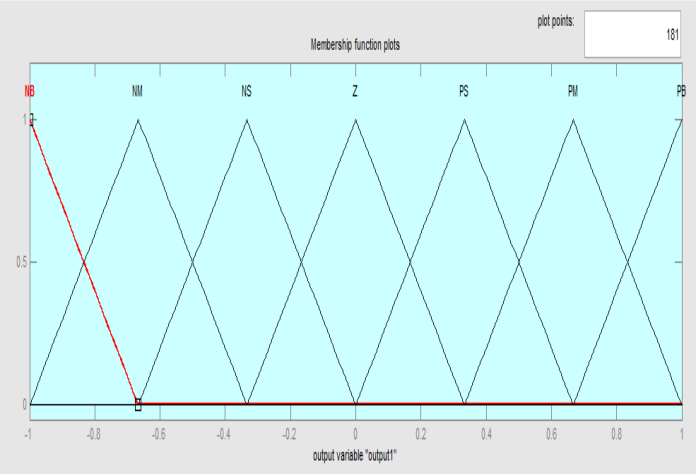

Fig. 11. Membership function used for input variable "Output"

Table 3: Fuzzy Rules

e/	NB	NM	NS	Z	PS	PM	PB
NB	PB	PB	PB	PM	PM	PS	Z
NM	PB	PB	PM	PM	PS	Z	NS
NS	PB	PM	PM	PS	Z	NS	NM
Z	PM	PM	PS	Z	NS	NM	NM
PS	PM	PS	Z	NS	NM	NM	NB
PM	PS	Z	NS	NM	NM	NB	NB
PB	Z	NS	NM	NM	NB	NB	NB

Based on the knowledge of the authors, the fuzzy system rules can be designed as shown in Table 3. ΔPpv and ΔIpv are the inputs while ΔIref is the output. The fuzzy inference of the proposed FLC is based on the Sugeno's method which is associated with the max-min composition.

2.5. In-phase voltage compensation method

In general, there are essentially three techniques deployed that include in-phase, the minimal energy injection method and presage so that DVR injection voltage maybe calculated. The paper basically discusses the in-phase compensation method deployed so that DVR.

The injection voltage can be measured, as it is simple in terms of the implementation and also quick responsive nature when computing the compensating voltage. The DVR capabilities enable it to compensate for the voltage drop through the process of injecting voltage through deploying the source voltage in the in-phase series injection transformer [21]. As in Figure 12, injected voltage in the secondary windings that runs through the series injection transformer is actually in the in-phase along with the supply voltage.

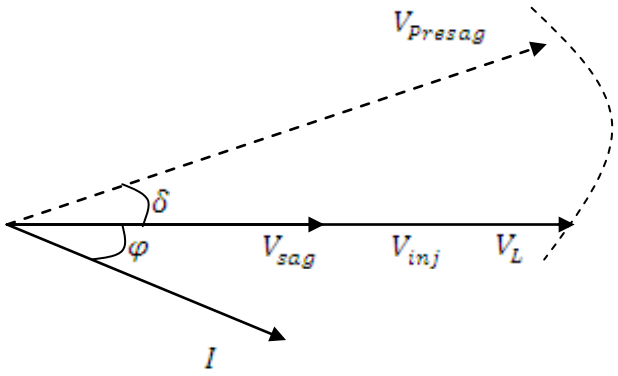

Fig. 12. In-phase compensation to presag voltage

In a state of normalcy, in an angle of zero phase, load and supply voltage (V are equal. At the time of voltage sags, the supply voltage decreases to a value less than or greater than the existing nominal value. As a result DVR counteracts to voltage sags and then injects required compensating in-phase voltage in along with the supply voltage so that the voltage may be restored to normalcy as at its nominal value. Injected DVR ( ) voltage may be expressed as follows:

$$|V_{inj}| = |V_{presag}| - |V_{sag}| \quad (9)$$

$$V_{DVR} = V_{inj} \quad (10)$$

$$|V_{DVR}| = |V_{presag}| - |V_{sag}| \quad (11)$$

Calculation of injected voltage angle may be done as per the following equation:

$$\angle V_{inj} = \theta_{inj} = \theta_s \quad (12)$$

Voltage Sag Detection using d-q transformation

is the supply voltage which gets transformed as positive sequence's d-q values in the proposed sag detection method. is acquired by deploying single-phase d-q transformation theory [22]. The component referred to as d which is part of the d-q transformation is equal to the DC value equivalent to the AC source voltage peak. Assuming that line voltage being the ideal sinusoidal waveform, the d-q theory assumes the generation of real and imaginary signal as follows:

$$V_{real}(t) = V_{smax} \sin(\omega t) \quad (13)$$

$$V_{image}(t) = -V_{smax} \cos(\omega t) \quad (14)$$

Here , is the real and imaginary part of , is the AC source voltage peak value. The d-q transformation can be expressed as

$$\begin{bmatrix} V_d \\ V_q \end{bmatrix} = \begin{bmatrix} \sin(\omega t) & -\cos(\omega t) \\ \cos(\omega t) & \sin(\omega t) \end{bmatrix} \begin{bmatrix} V_{real} \\ V_{image} \end{bmatrix} \quad (15)$$

From the transformation as shown above, the following values are obtained, V_d = and = 0. There is an inherent delay that is an outcome under natural circumstances; however the delay is minimal in comparison to system response under voltage swells, sags or outages. Monitoring of , returns the voltage drop and rise and the manipulation of Vq will return the initial phase jump information.

3. Simulation Results

This Simulation of the proposed work has been carried out in MATLAB. Results from the simulation have further been evaluated. During the initial phase park transformation results have been evaluated.

is the distorted voltage where the voltage suddenly drops which can lead to SAG voltage.

Fig. 13 shows the voltage sag compensation of the conventional PI and proposed system in DVR mode. In DVR mode, the proposed system acts as DVR wherein the voltage sag is compensated in the presence of input AC supply.

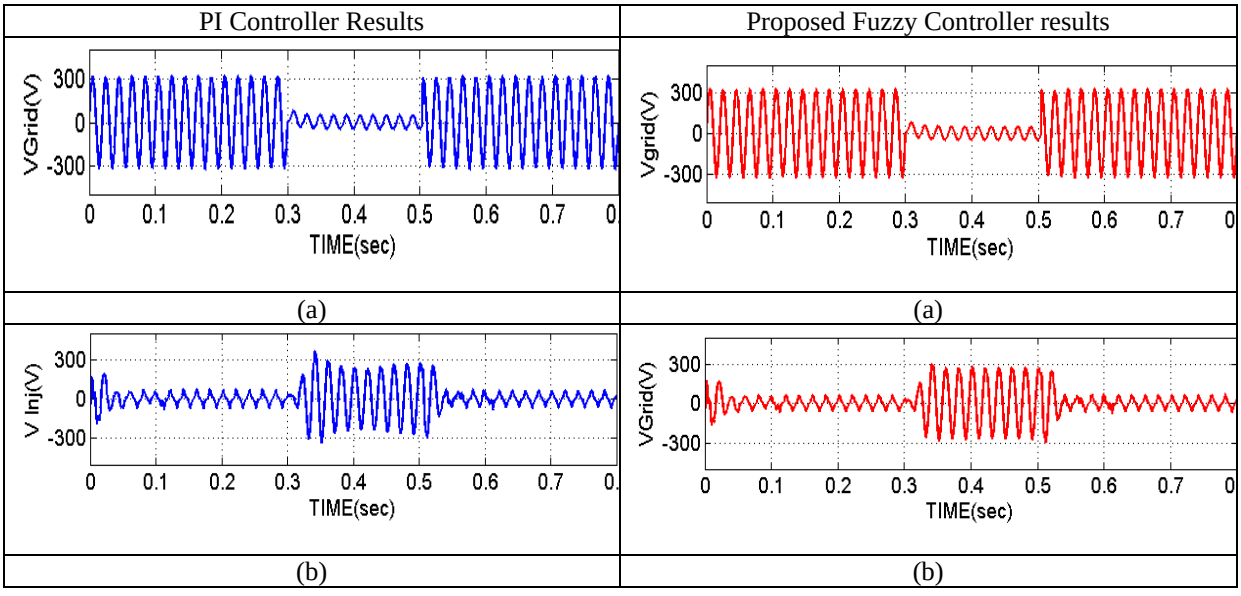

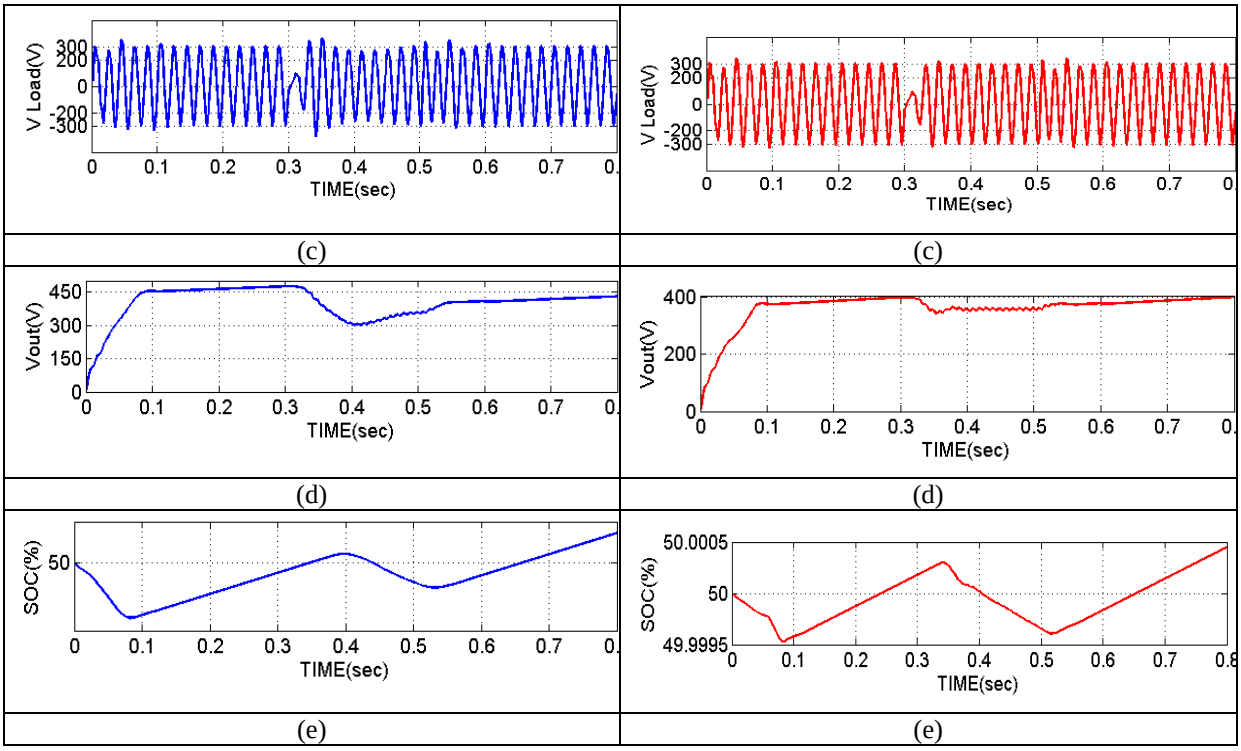

Fig. 13. Evaluation results of proposed system in (1) DVR Mode

Fig. 13 shows the resultant waveforms of the proposed system as a DVR. Figure 13 (a) shows the grid voltage waveform of both the PI and proposed fuzzy controller system. It is observed from the figure that, at time 0.2 second, voltage sag of 50

observed in the system. So, this implies that, 250 to be injected in the system to compensate the

voltage sag. This injected voltage waveform of the both PI and fuzzy controller is clearly shown in Fig 13 (b). Fig 13 (c) shows the load voltage waveform of the both PI and fuzzy controller at the voltage sag condition. It is observed that, at 0.2 second, there is sudden drop in load voltage due to the voltage sag. But, suddenly at 0.23 second, the voltage sag is compensated due to the injected voltage. Fig 13 (d) shows the output voltage wavwform of the both PI and fuzzy controller of the system. Fig 13 (e) shows the State Of Charge (SOC) battery of the both PI and fuzzy controller at the voltage sag condition. It is clearly shown that, at the voltage sag condition, the battery is in discharging condition from (0.2 to 0.4 seconds). The battery operates in charging condition except in sag condition. Hence it can be said that, the proposed fuzzy controller approaches provides better performance when compared with the existing PI controller system.

Table 4: Converter Load Voltage comparsion

Methods	Load Voltage		
	Peak Overshoot	Peak Undershoot	Settling Time
Fuzzy Controller	22 V	2 V	0.384 sec
PI Controller	66 V	31 V	0.46 sec

Table 4 clearly shows the performance of the proposed fuzzy controller approach in terms of peak overshoot, peak undershoot and settling time. It is observed from the table that the proposed fuzzy controller approach attains peak overshoot at 22 volts, peak overshoot is 2 V and settling time at 0.384 seconds where as the peak overshoot, peak undershoot and settling time of the conventional PI controller is observed to be higher. Fig 14 shows the graphical representation of this comparison.

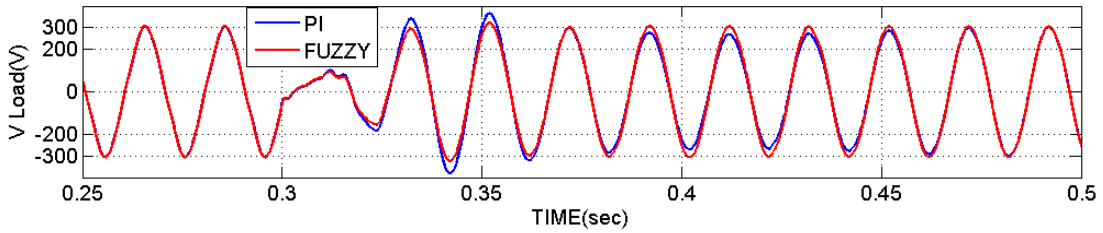

Fig. 14. Load Voltage Comparision

Table 5: Converter Output Voltage comparsion

Methods	Converter Output Voltage		
	Peak Overshoot	Peak Undershoot	Settling Time
Fuzzy Controller	-	9 V	0.384 sec
PI Controller	-	50 V	0.46 sec

Table 5 clearly shows the performance of the proposed fuzzy controller approach in terms of peak overshoot, peak undershoot and settling time. It is observed from the table that the proposed fuzzy controller approach attains peak overshoot at 9 volts and settling time at 0.384 seconds where as the peak overshoot and settling time of the conventional PI controller is observed to be higher. Fig 15 shows the graphical representation of this comparison that has been drawn.

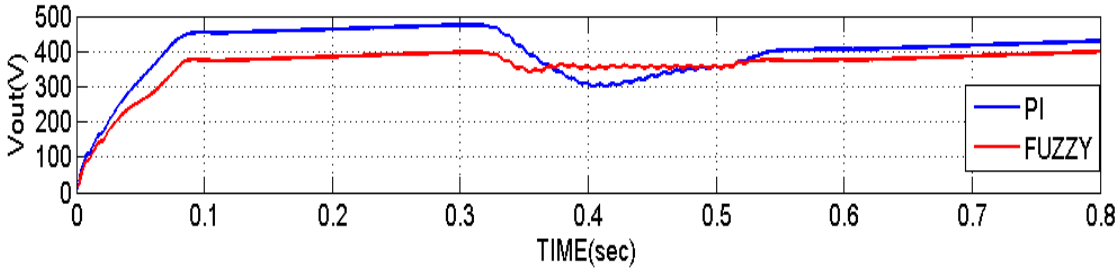

Fig 15. Output Voltage Comparison

Fig 16 shows the SOC comparison of PI and proposed fuzzy controllers. It is to be observed that, the proposed Fuzzy controllers show better performance when compared with the conventional PI controller.

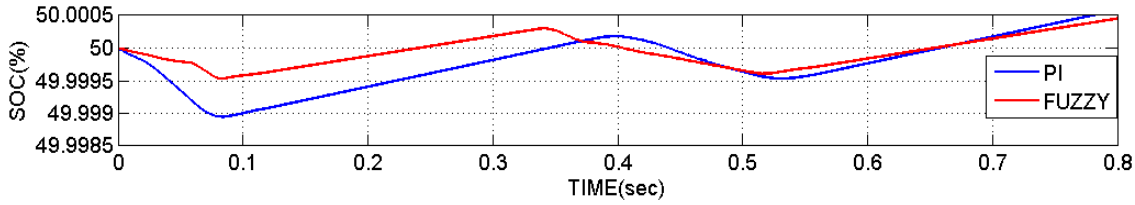

Fig.16. SOC comparison of converters

4. Experimental Results

A TMS320C6713 digital processor is used as the controller. The hardware setup was accomplished with a 110 V DVR prototype to experimentally verify the feasibility of implementation of the proposed PV-DVR. This prototype consists of a solar panel, low and high step-up DC–DC converter, batteries, single phase series injection transformer and a load.

Table 6: The parameters of the experimental setup

S. No	Description	Specification
1	Panel voltage V_{PV}	48V
2	Panel current I_{PV}	2.56A
3	Panel power P_{PV}	122.8W
4	Battery voltage V_{BAT}	48 V

5	Converter output voltage V_{out}	176 V
6	Coupled Inductor ETD-59-core pc-40	Np:Ns=1:4
7	Capacitors	C1=C2= 56 µF/ 100V C3=C4= 22 µF/ 300 V C0= 180 µF/ 450 V
8	Nominal Grid Voltage	110 Vrms

A tap changing transformer is used to introduce the voltage sag and outages on the system. The inverter is a standard H-bridge system that is connected at the 110 Vrms level through a 1 kV A single phase injection transformer. SPWM modulation technique is used to implement the switching of MOSFETs (IRFP460). The DC bus voltage can be charged up to 176 V using the PV and rectifier output voltages. For all experiments the line frequency was 50 Hz, the inverter switching frequency was set to 4 kHz and proposed bidirectional converter switching frequency of 10 kHz. The storage batteries of eight 6 V, 4.5 Ah is connected in series. The parameters of the experimental setup are shown in Table 6.

The experimental results of two different voltage levels are presented. Two sets of experiments were conducted to validate the proposed topology, which are all analyzed in the following subsections. The grid voltage, DVR injected voltage, load voltage, Input converter current Iin, battery current Ibat, Converter Output Voltage Vout and Gate pusles GS1, GS2 and GS3 for switches S1, S2 and S3 respectively. The above mentioned specifications are measured by Digital Signal Oscilloscope (DSO), is presented.

In this experimental validation, nominal grid voltage considered is 110 Vrms. Two voltage sag conditions have been considered for this experimental verification.

For all experiments a pure resistive load of 110 ohm is used. Fig 17 (a) and 17 (b) shows the converter input current and the gate pulse for switch s1 respectively. The converter input current is 2.56 A.

Case 1: Voltage Sag condition with 86.28 Vrms

Fig 17 (c) shows the supply voltage drops to 21.56% (24 Vrms) of its nominal value.

Based on the voltage sag created, the voltage is injected through the proposed DVR which compensates the sag condition. Fig 17 (a), (b) and (c) clearly shows the grid voltage, injected voltage and the load voltage for case 1.

The PV power maintained for this experimental set up is 122.8 W as shown in table 2. Now, in order to inject the voltage for the 21.54% sag condition, 48.28 W power is required. Since, PV power is surplus, the remaining 69.12 W is stored in the battery.

Due to the surplus PV power, Switch S2 is in ON condition and the remaining power is stored in the battery which is clearly depicted in Fig17 (c) and 17 (d). The DC bus voltage (Vout) is maintained constant at 176 V as shown in Fig 17 (e)

.

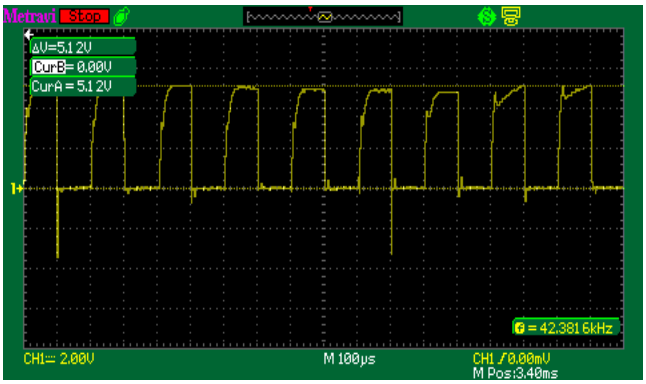

(a)Converter Input Current

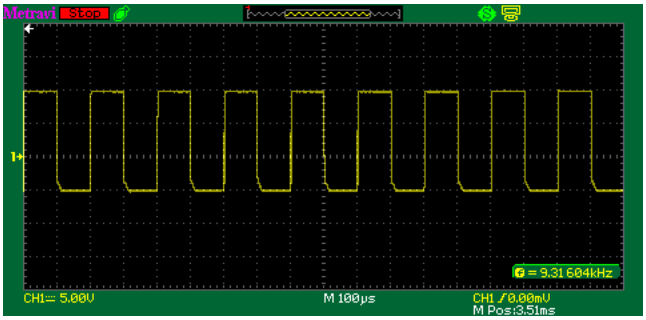

(b) Gate pulse for Switch S1

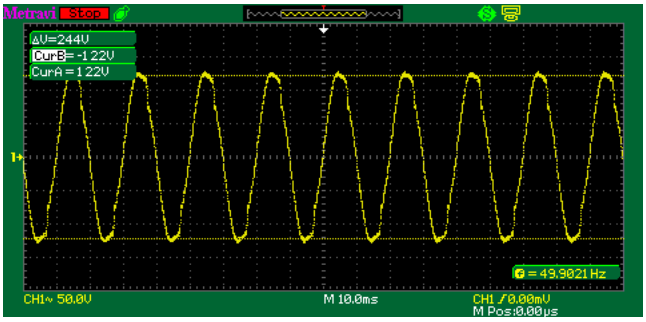

(c) Grid Voltage

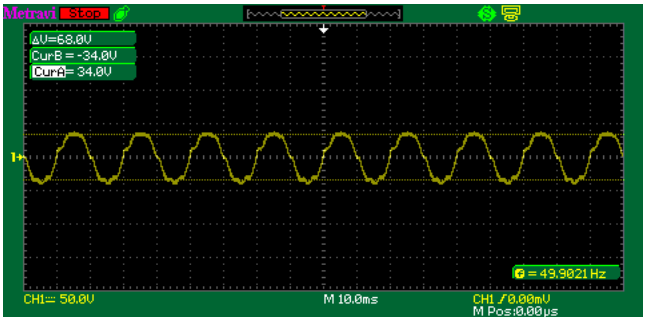

(d) Injected Voltage

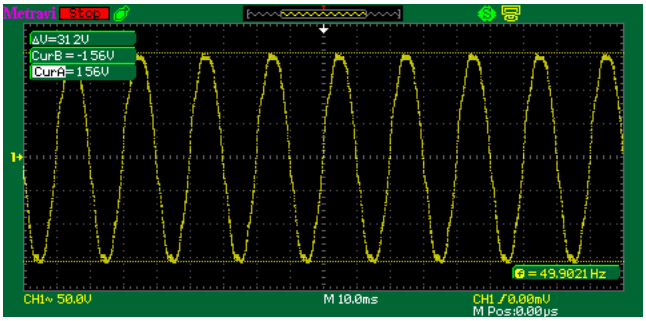

(e) Load Voltage

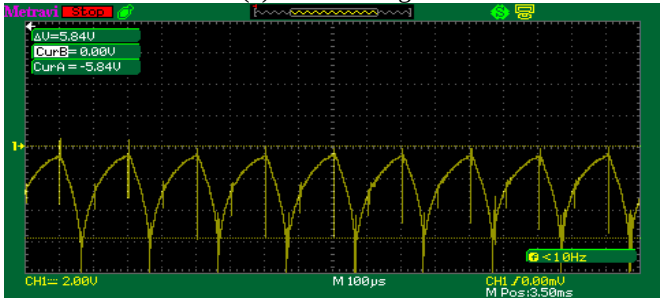

(f) Battery Current

Case 2: Outage compensation

In this case, the proposed PV-DVR is tested during an outage condition. The 0% of nominal voltage is applied to the system by disconnecting the grid voltage. Fig 18.(a), (b) and (c) clearly shows the grid voltage, injected voltage and the load voltage for case 2.

In this scenario, there is no PV power, so, the required power is discharged from the battery to support the load demand as depicted in Figure 18(d). In order to make the battery discharge, switch S3 has to be in ON condition which is depicted in Fig 18 (e). The DC bus voltage (Vout) is maintained constant at 166 V as shown in Fig 18(f).

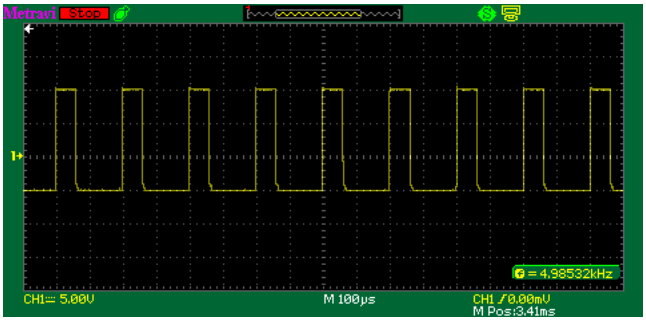

(g) Gate pulse for Switch S2

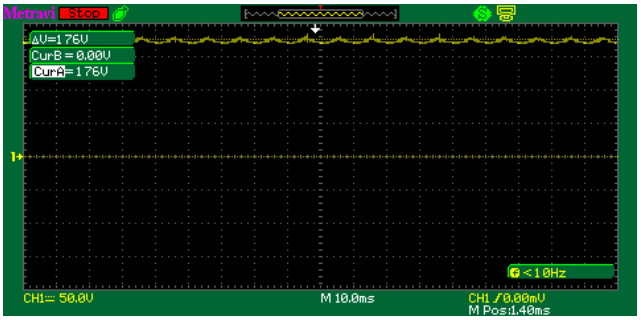

(h) Converter Output Voltage

Fig.17: Voltage Sag condition with 86.28 Vrms

5. Conclusion

This paper presents a novel approach and application that deploys a PV solar system to address voltage swells, sags and outage improvement through DVR for both residential and small scale industrial purposes. A novel TPHGC with single battery charging bidirectional conversion operation has been proposed in this work to overcome the limitation of the existing DVR system. The PV-DVR has been designed such that it reduces energy consumption from the main utility grid by basically detaching the utility grid from the load using several semiconductor switches. This is carried out once the PV array produces real power that is an equivalent amount or in excess in terms of the required load demand. Additionally, it has a twofold benefit as it reduces panel tariff and also aids in avoiding UPS and stabilizer use for personal individual residential use, small scale industrial purposes and at other educational institutions. The results from the experiments conducted and the simulation process show PV-DVR capability in terms of mitigating variations in voltage.

6. References

[1] J.Pedra, L.Sáinz, F.Córcoles, and et al, Symmetrical and unsymmetrical voltage sag effects on three-phase transformers , IEEE Transactions on Power Delivery, 20, 2005, pp.1683–1691.

[2] J.Arrillaga, M.Bollen, and N.Watson, Power quality following deregulation, IEEE proceedings , 8, 2008, pp.246–260.

[3] J.F.Moon, S.Y.Yun, and J.C.Kim, Quantitative evaluation of the impact of repetitive voltage sags on low-voltage loads, IEEE Transactions on Power Delivery, 22, 2007,pp.2395–2400.

[4] M.H.J.Bollen, What is power quality, Electric Power Systems Research, 66, 2003, pp.5–14.

[5] A.Moreno-Munoz, J.J.G.de-la-Rosa, M.A. Lopez-Rodriguez, and et al., Improvement of power quality using distributed generation, International Journal of Electrical Power Energy System, 32(10), 2010, pp.1069–76.

[6] M.Ashari, T.Hiyama, M.Pujiantara, and et al.: 'A novel dynamic voltage restorer with outage handling capability using fuzzy logic controller', In: Proc innovative computing, information and control conference, 2007, pp. 51.

[7] S.Sasitharan, M.K.Mishra, B.Kalyan Kumar, and et al, Rating and design of DVR injection transformer, International Journal of Power Electron, 2, (2), 2010, pp.143–63.

[8] F.A.L.Jowder, Modeling and simulation of different system topologies for dynamic voltage restorer using simulink, In: Proc electrical power and energy conversion systems conference, 2009, pp. 1–6.

[9] J.H.Han, I.D.Seo, J.G.Shon, and et al, Development of on-line type dynamic voltage compensation system using super capacitor , In: Proc power electronics conference, 2007, pp.455–60.
[10] R.Omar, and N.A.Rahim, Voltage unbalanced compensation using dynamic voltage restorer based on super capacitor, International Journal of Electrical Power Energy System, 43,2012, pp.573–81.
[11] A.O.Al-Mathnani, A.Mohamed, and M.A.Mohd Ali, "Photovoltaic based dynamic voltage restorer for voltage sag mitigation", In: Proc of 5th student conference on research and development, 2007, pp.1–6.
[12] M.Ramasamy, and S. Thangavel, Experimental verification of PV based Dynamic Voltage Restorer (PV-DVR) with significant energy conservation, Electrical Power and Energy Systems, 49,2013, pp.296–307.
[13] N.Mohan, T.M.Undeland, and W.P.Robbin, Power electronics converters, applications and design, John Wiley & Sons Asia Pvt Ltd, 3rd edition, 2006, pp. 172–178.
[14] Y.P.Hsieh, J.F.Chen, T.J.Liang and et al, Novel high set-up DC–DC converter for distributed generation system, IEEE Trans Ind Electron, 60(4), 2011, pp.1473 - 1482.
[15] A.R.Reisi, M.H.Moradi, and S.Jamasb, Classification and comparison of maximum power point tracking techniques for photovoltaic system: A review, Renew. Sustain. Energy Rev, 19, 2013, pp.433–443.
[16] N.Femia, G.Petrone, G.Spagnuolo and et al, Optimization of perturb and observe maximum power point tracking method, IEEE Trans. Power Electron, 20, 2005, pp.963–973.
[17] D.Lalili, A.Mellit, N.Lourci, and et al, Input output feedback linearization control and variable step size MPPT algorithm of a grid-connected photovoltaic inverter, Renew. Energy, 36, 2011, pp.3282–3291.
[18] H.Altas, and A.M.Sharaf, A photovoltaic array simulation model for MATLAB simulink GUI environment, In: Proc Clean Electrical Power Conference, 2007, pp.341–345.
[19] Z.M .Salameh, F. Dagher, The effect of electrical array configuration on the performance of a PV powered volumetric water pump, IEEE Trans Energy Convers, 5, 1990, pp. 653–658.
[20] A.A. El-Tayyan, PV system behavior based on datasheet, Journal of Electron Devices, 9, 2011, pp.335–341.
[21] T.I.El-Shennawy, A.M.Moussa, M.A.El-Gammal, and et al, A dynamic voltage restorer for voltage sag mitigation in a refinery with induction motors loads, Am J Eng Appl Sci, 3(1), 2010, pp.144–151.
[22] J.Lira, C.Nunez, M.Flota and et al, Control strategy to improve voltage sag ride through in single phase multilevel active rectifier, In: Proc electrical and electronics engineering, 2006, pp.1–4.